The tensile testing of individual wood fibers using environmental scanning electron microscopy and video image analysis

Laurence Mott, Stephen M. Shaler, Leslie H. Groom, and Bei-Hong Liang

ABSTRACT: Relationships between virgin fiber types, fiber production techniques and mechanical properties are well understood and documented. For recycled fibers, however, these same relationships are confounded by unquantified degrees of further mechanical and chemical damage. To gain a more comprehensive understanding of the impact of recycling on secondary fibers, the potentially deleterious effect of recycling upon fiber mechanical properties must be quantified. In this study, individual fibers—both recycled and virgin—were tested in tension with an environmental scanning electron microscope. Failure characteristics of both recycled and virgin fibers are reported. The influence of both natural and processing induced gross defects were seen to be highly influential in controlling mechanical behavior. The importance of defects and the implications for modeling the behavior of fibers is explained.

KEYWORDS: Ecology, image analysis, mechanical properties, reclaimed fibers, recycling, scanning electron microscopy, television, tensile tests, wood fibers.

Relationships between virgin fiber types, fiber production techniques and mechanical properties are well understood and documented *(1)*. For recycled fibers, however, these same relationships are confounded by unquantified degrees of further mechanical and chemical damage *(2)*. Quantifying recycling effects on pulp quality has previously been a matter of interpreting the results of laboratory paper testing. This method of study has now largely established the effects that recycled pulps have upon paper quality *(3)*. Recently, however, individual fiber tests have led to more detailed information concerning the properties of specific pulp fibers at various stages in the recycled fiber life cycle *(4)*. Methods used to obtain individual virgin fiber properties and also recycled fiber properties give an insight into the changes that occur in secondary fiber properties after a varying number of recycling runs. Individual fibers are subject to recycling related alteration, but it is apparent that testing procedures have impacted highly on previously obtained data *(5,6)*. Wuu *et al.* *(4)* speculate that the restrained drying mechanism, frequently used in the preparation of tensile test fiber samples, enhances individual fiber properties through the partial removal of free-drying induced microcompressions, originally described by Page and Tydeman *(7)*. Such drying also reduces strain to failure by removing latency in the form of gross defects such as kinks, crimps, and curl *(8)*.

It is not surprising therefore, that restrained drying has a tendency to increase initial modulus values. These are then believed to gradually decrease upon further recycling *(4)*. Decreasing modulus values are accompanied by increasing strain to failure. Both phenomena presumably occur as a response to the further kinking, crimping, curling, and micro-compressional damage to the fiber. This damage it would seem is

Mott, Shaler, Groom, and Liang are, respectively, research assistant and associate professor, Dept. Forest Management, University of Maine, Orono, ME 04469-5755, senior research scientist, USDA Southern Forest Products Experiment Station, Pineville, LA 71360, and former research assistant, Dept. Forest Management, University of Maine, Orono.

1. Tensile testing stage and fiber gripping system designed to fit in the ESEM chamber

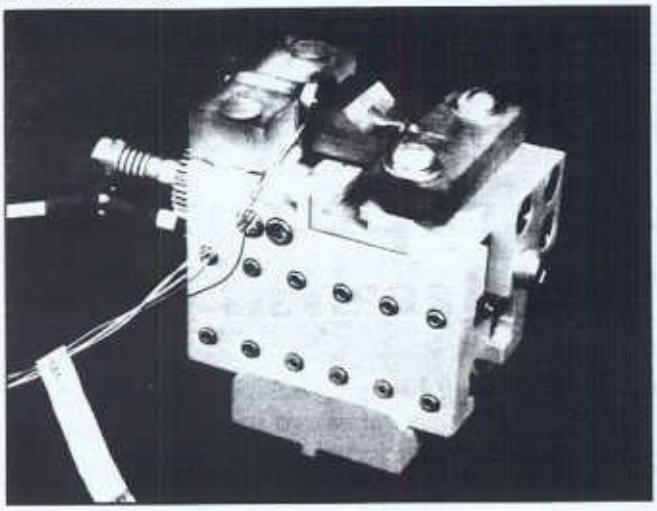

2. ESEM photomicrograph showing crack propagation through a single virgin linerboard fiber. Crack initiation at pit (load = 7.7 g)

largely the result of the fiber drying in a free or semi-free state during the recycling process. This theory supports the work of Kim *et al. (9)*.

Due to the nature of individual fiber testing, it has previously been impossible to directly quantify the impact that regions of fiber microcompressions or associated recycling/drying defects, such as crimps, curls, and kinks, have upon the overall mechanical potential of individual fibers. Page and El-Hosseiny *(10)* made use of a statistical approach in an attempt to relate individual fiber gauge length to the presence of these randomly induced defects, and further work of Page and Seth *(8)* theorized the relative shape of load elongation curves for individual fibers containing specific defect types. However, the relative impact defects have upon fiber properties still requires investigation, and with little specie specific data presently available, generalizations concerning the potentially damaging effects of recycling on individual secondary fibers must still be avoided.

This study attempts to address this issue, by quantifying the impact that visible potential strength reducing defects have upon the overall mechanical properties of individual fibers. This report will briefly outline a new fiber testing procedure currently under development. Also presented, in micrograph form, are partial results of an investigation into fiber failure characteristics. Other aspects of the study, e.g., a quantitative analysis of strains in the vicinity of fiber defects and ultimate load capabilities, are currently under way.

A new method to study fiber failure mechanisms

In order to advance the knowledge of secondary fiber properties the development of a new fiber testing method was regarded as essential. An environmental scanning electron microscope (ESEM) was used to observe individual dynamic fiber tensile tests. The ESEM was fitted with a modified tensile stage capable of incorporating a load monitoring mechanism and a fiber gripping assembly. The resulting images could then be interpreted with the aid of an image analysis system.

Previously, the only fiber tensile tests to use any type of optical analysis were those developed by Page *et al. (11)*. A cine camera mounted to a polarizing light microscope was used to record fibers under dynamic load. The images obtained were later used to verify the occurrence and influence of crystalline or fibrillar disruptions in individual fiber specimens. Cine stills were also used to determine whole gauge length strains. However, technological restraints limited the usefulness of this technique and the detection or quantification of highly localized strains surrounding microcompressions or defects was impossible. Dynamic imaging of actual failure sequences using this form of microscopy was also difficult. The most common form of failure characterization has been to carry out microscopic investigations following fiber failure. Armstrong *et al. (12)* made use of SEM to investigate fracture surfaces. Surfaces were found to be useful in determining whether defects contributed to failure and could also be used to measure the S2 microfibrillar angle.

Benefits of environmental scanning electron microscopy

An ESEM permits the type of high resolution, high magnification, and large depth of field imaging associated with standard scanning electron microscopy (SEM), while simultaneously allowing biological materials to be observed in their natural state. ESEM differs from standard SEM in that the sample is not viewed under a high vacuum. Instead, a gas, generally water vapor, is introduced into the chamber as air is expelled. Unlike a standard SEM, the column housing the gun and specimen chamber is divided into a series of differential pressure zones; separated by

3. Crack enlargement through S1 and S2 (load = 8.6 g)

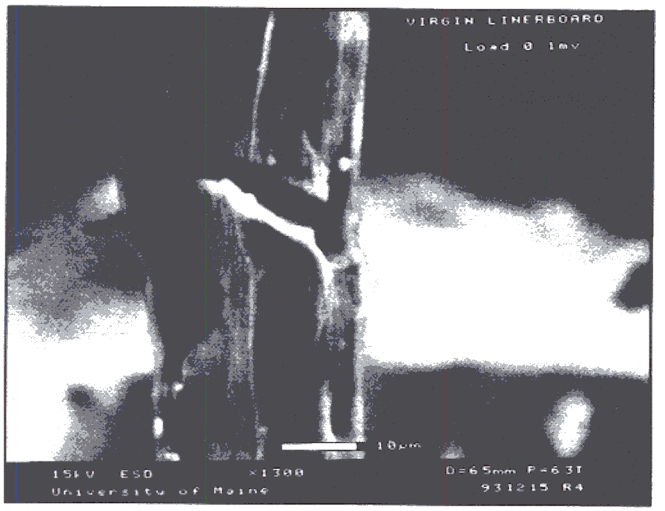

4. Virgin linerboard fiber fracture surface (ultimate load = 9.5 g)

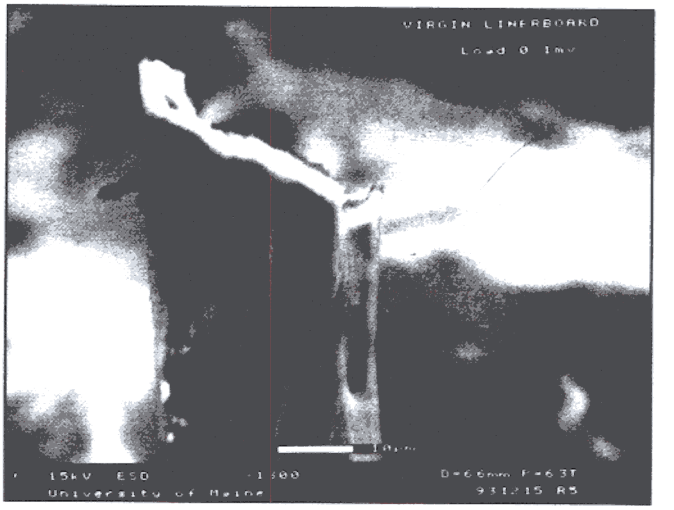

a series of pressure limiting apertures. This allows the electron gun to remain under a high vacuum while the sample chamber may contain a gas. The conventional Everhart-Thornley secondary electron detector is replaced by a detector that uses this gas as an amplifier. The gaseous environment in the chamber serves two purposes. First, it prevents the build-up of charge on the surface of insulating specimens, thus removing the need for conductive coatings. Secondly, where water vapor is used as the gas, wet or damp specimens may be viewed in their natural hydrated state. If the chamber pressure is maintained at 5–20 torr and the specimen temperature between 0–22°C, (conditions depend on the sample) it is possible to image biological samples under saturated water vapor conditions *(13)*. Under such conditions, samples do not gain moisture by condensation or lose moisture through evaporation. This makes it possible to image dynamic processes in the ESEM under a range of environmental conditions.

Microtensile testing stage

A Microtensile testing stage designed to fit inside the ESEM chamber was provided by Electroscan. It was subsequently heavily modified to permit the tensile testing of individual wood fibers. The stage itself has a dual cross-head type movement to aid in keeping areas of interest centrally located on the viewing monitor while load is applied. The gripping system, shown in **Fig. 1**, was based upon Kersavage's *(5)* fiber testing method, where the fibers are held encastre via a ball and socket joint (a drop of adhesive providing the ball attached near the ends of the fiber), rather than held rigidly with adhesive. This system has been proven to minimize the problems of fiber misalignment, which can lead to premature failure *(5)*. It also facilitates the rapid replacement of fibers once they have ruptured (approximate 3–5 min change over), thus ensuring a substantial number of fibers can be tested. A modified miniature 1-lb load cell was incorporated into the test grips. The diaphragm type design of the load cell necessitated modifications. Sealed load cells have air entrapped in them, rendering them sensitive to fluctuating air pressure, which has to be accounted for during calibration. Without modification the pressure variations in the ESEM would continually lead to a false load reading. The load cell was modified to ensure it was nonhermetically sealed. A vacuum sealed inlet/outlet port in the ESEM chamber wall permits load readings to be taken externally via a voltmeter, as the tensile test progresses.

Fiber preparation

It is clear that fiber preparation methods impact greatly on individual fiber mechanical properties *(5,6)*. To minimize this effect and to prevent more than a nominal straining of fibers prior to tensile testing, a handling procedure similar to that adopted by Kim *et al. (9)* was used in this study. Virgin wood fibers consisted of commercial kraft linerboard loblolly pine (*Pinus taeda* L.) pulp samples obtained in a never dried, chilled wet state while recycled fibers consisted of office waste and old newsprint that had been pulped in a Hydrapulper. Single fibers extracted from a dilute suspension, using fine forceps, were placed in individual water droplets between standard glass slides. To avoid potential damage to the central span of the fiber samples, only the very ends of the fibers were handled with the forceps. Approximately 10 fibers were applied to each glass slide. The second glass slide was applied to control drying rate and to prevent excessive fiber twisting and curling. The fibers were then allowed to dry under ambient conditions.

Dried fibers were removed from the slides and prepared under a dissecting microscope to ensure selected samples were free from preparation-induced defects. Individual fibers were laid across a prepared channel,

5. ESEM photomicrograph showing crack propagation through a single mixed office waste fiber. Crack initiation at a point of kinking and compressive flattening (load = 4.5 g).

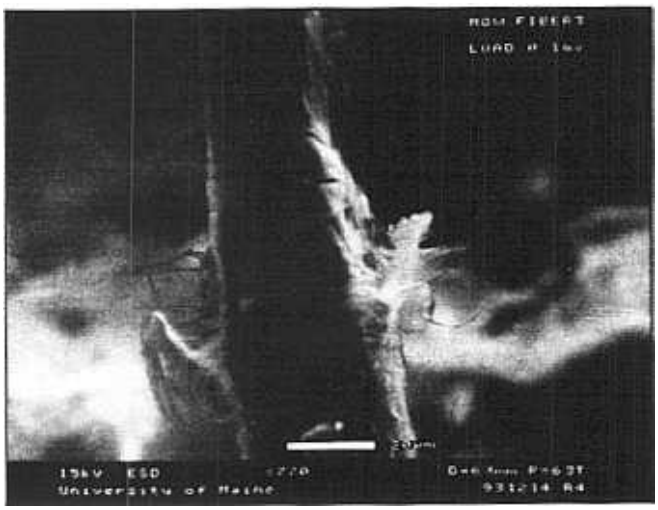

6. Crack enlargement (load = 8.6 g)

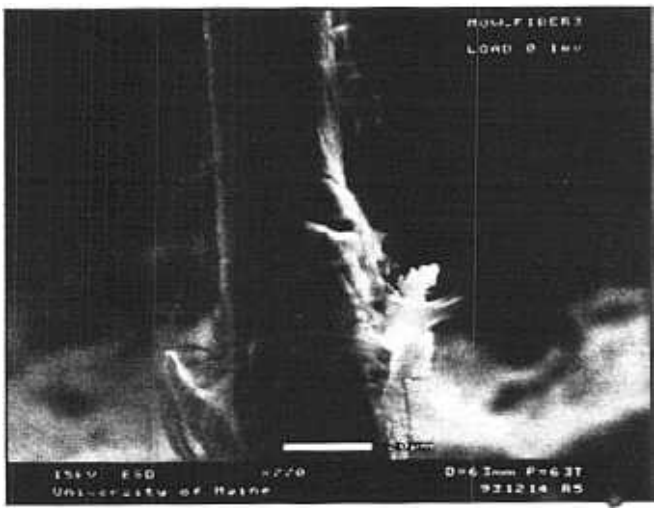

with only the very ends of the fibers used to support the central span. A two-component epoxy was mixed and single spherical droplets were applied close to both supported ends using fine forceps. This technique is similar to that described in detail by Kersavage *(5)*. The resulting fiber consists of an untouched central span with an epoxy droplet attached close to either end. The spherical droplets then served as ball joints in the described ball and socket fiber gripping assembly.

Tensile testing procedure

The modified tensile stage (shown in Fig. 1) was attached to the X,Y,Z stage of the ESEM. Once a fiber had been placed into the gripping system, the XYZ controls were used to manoeuvre the fiber gripping device into the beam path/field of view. The individual fiber could be clearly seen on the video monitor. Prior to tensile testing, at magnifications of approximately 700X, each fiber was scanned along its length to assess where the point of failure was most likely to occur. This scanning process also permitted the fiber to equilibrate to the moisture conditions present within the ESEM chamber while not under load. The initial images displayed in **Figs. 2 and 3** give an indication of the type of defects that were of interest. Adjusting the microscope parameters to focus on this potential weak point, the fiber was then strained at a crosshead movement rate of 1 μm/s. After testing several virgin fibers, it became possible to select the point of failure prior to testing. Selecting a potential failure point for secondary fibers proved to be easily done. It should be noted that beam condenser strength was adjusted to prevent damage to the surface of the fibers at very high magnifications. However, prolonged exposures, i.e., over 10 min continually focused on one region, can leave small score lines on the fiber wall. Beam damage was not deemed to have any effect on strength values or failure characteristics of the fibers.

Recording mechanism and digital image analysis

Several tensile test visual recording mediums are presently used. Super-VHS video is used to record all fiber loading tests. Videoing the tests serves two purposes. First, a review of the video tape can yield further valuable information with regard to respective positions and points of fracture initiation. Secondly, it permits post processing of the video images. Through a technique known as digital image correlation (DIC), previously applied to investigations such as measurement of strain in paper and wood *(14,15)* still images captured from video tape can be used to calculate strains within highly localized fiber regions. When used to analyze fiber images magnified approximately 1000X, it is possible to quantify strains surrounding pit fields, microcompressions and gross defects. At higher magnifications initial studies suggest that displacements will be measurable to within at least 0.4 μm. A subsequent paper will report on these findings.

Individual RGB (non-interlaced) format images taken from the monitor can also be captured digitally via a frame grabber. The resulting images are of a higher resolution and contain less random noise than those retrieved from video tape. For this reason, digitally recorded images are particularly desirable for digital image correlation work. The final image recording medium used is the standard Polaroid photomicrograph. Due to the time required to expose each print, photomicrographs are only taken where publishable quality images are required. The images displayed in this study are reproduced from Polaroid photomicrographs.

7. Crack direction change (load = 10.9 g)

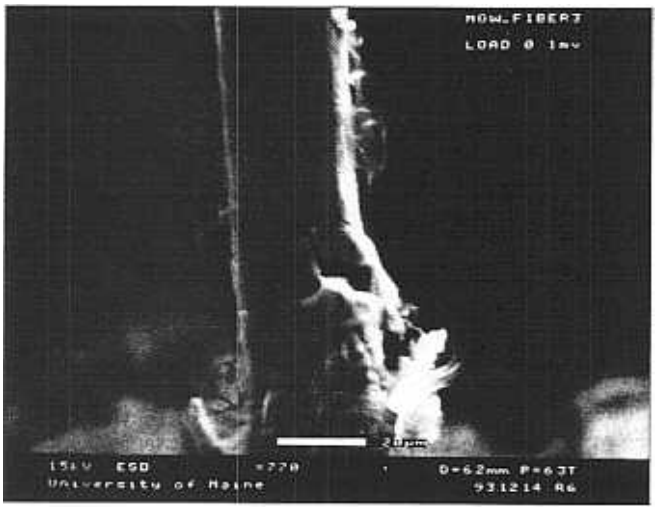

8. Mixed office waste fiber fracture surface (ultimate load = 11.4 g)

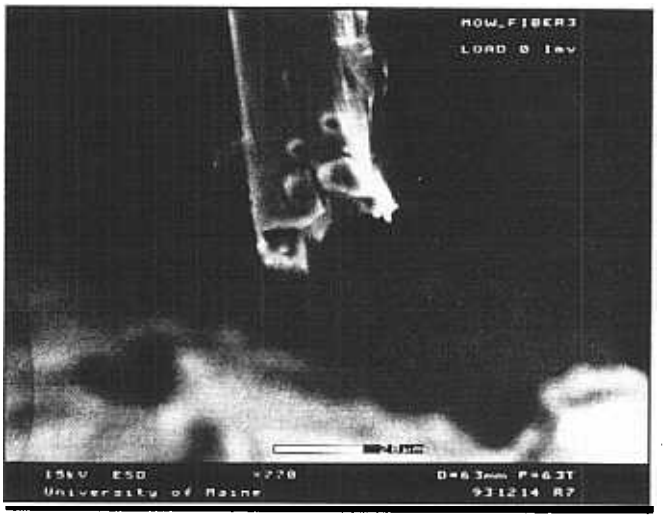

Preliminary results and discussion

The images displayed in **Figs. 2 through 8** represent failure characteristics commonly found to be associated with virgin and secondary fiber types. Largely undamaged virgin softwood fibers were seen to fail in tension at points of natural stress concentrations. Not surprisingly these stress concentrations occur in the locality of pit fields, where large variations in the S2 microfibrillar angle have been proven to exist *(16)*. Recorded observation of 65 fibers also suggested that virgin wood fibers infrequently fail at points where there is no gross natural defect. The critical defect generally exists in the form of the largest noticeable bordered pit. Even where noticeable processing induced defects exist in the virgin fibers tested (a series of microcompressions is a good example of such a defect), the failure primarily occurred at the location of the most obvious natural structural weakness—the bordered pit. This makes the point of failure relatively easy to pinpoint. In heavily pitted areas, the region of failure initiation was most prevalent where two pits are located side by side. Page *et al. (11)* was able to establish the relationship between the presence of natural defects such as pits, induced defects such as microcompressions, and the premature failure of fibers at these sites. However, Page *et al. (11)* were unable to directly define the exact location of crack initiation due to technological limitations. This technique confirms the findings of Page *et al. (11)* but also permits high magnification, high resolution, and direct imaging of surface feature related failure mechanisms. This permits pit-related failure to be further classified.

The fracture surface can be observed to run either directly through the pit itself, effectively halving the pit aperture and chamber, or more commonly in a plane directly adjacent to the pit, from a point just above or below the vicinity where cell wall thickening would be seen to occur.

These findings may have implications with regard to modeling fiber tensile behavior. It is apparent that it is no longer sufficient to consider wood fibers as perfect cylinders or flattened rectangular tubes *(1,17)*. The impact of natural defects needs to be considered in greater detail. What can be loosely described as generic strength reducing microcompressions and pitting (of varying degrees of severity) must be taken into consideration, but they must not be regarded as the only major ultimate tensile stress/modulus limiting factor *(11)*. Microcompressions and pits no doubt contribute to the premature failure of virgin wood fibers as compared to their predicted ultimate tensile stress, but observations from this study indicate that the major limiting factor is likely to be S2 microfibrillar angle deviation found in the highly localized pit field regions.

Recycled fibers display a similar response under tensile loading. Failure is seen to occur primarily in the regions where the greatest S2 microfibrillar disruption has taken place. Like virgin fibers this is usually in the region of the largest natural defect. However, of the limited number of samples actually tested and recorded (38 fibers), it was found that processing induced defects also impacted the most common point of secondary fiber failure.

Impact of defect types on recycled fiber properties

A tear in the fiber wall is the most severe defect a fiber can sustain and still bear an appreciable load. It was observed that even a seemingly minute tear can be catastrophic should it penetrate the S2 layer, thus initiating premature fiber failure. Regions of the cell wall that have become compressively flattened, as

opposed to collapsed which is relatively common, were observed as the regions in which failure will otherwise occur if the fiber is gross-defect free. Severe microcompressions or dislocations that obviously run through the entire fiber structure, and which do not pull-out under load, are also seen to be the precursors of fiber fracture/rupture. It is also interesting to note that secondary fibers visibly free of these defects but also probably containing many smaller microcompressions were observed to fail in the vicinity of pit fields and infrequently in clear sections of fiber wall, even if prolifically microcompressed.

Fracture behavior of secondary and virgin fibers

The limited number of fiber test observations indicated that recycled fibers and never recycled virgin fibers may behave differently under tensile load. Recycled fibers appear to take longer to fail following crack initiation than virgin fibers when a constant load is maintained. Even from a limited number of observations, it was obvious that during crack propagation, the width of the crack often grew significantly wider in recycled fibers than in virgin fibers. It is proposed that recycled fiber intra-cellular wall delamination may be the cause of this. Partial or total separation of the S1 layer from the S2 in the failure region would allow the S1 layer to fail well in advance of the S2 as load is applied. To the observer, this appears as a large crack opening in the fiber wall prior to catastrophic or total failure. A structurally sound nondelaminated virgin fiber would strain at a constant rate both in the S1 and S2 until the point of rupture—a virtually simultaneous action across the whole secondary wall. Dynamic observations of secondary fiber S1 layer delamination and exaggerated crack width support SEM and transmission electron microcroscopy findings of Okayama *et al. (18)* who report a gradual peeling of the S1 during progressive recycling. It is suggested that this may be due to the effect of differential shrinkage between the S1 and S2 layers.

Conclusions

1. Pit fields were observed to be the most influential defect with respect to controlling the position of fracture in virgin fibers. Microcompressions were also seen to dictate the position of virgin fiber failure in a limited number of cases, specifically where microcompressions could be seen as the most obvious structural flaw in the absence of visible pitting. Dynamic observations are able to clearly confirm that pit failure can be further classified into two types: fracture running either directly through the pit itself, effectively halving the pit aperture and chamber, or more commonly in a plane directly adjacent to the pit, from a point just above or below the vicinity where cell wall thickening is seen to occur.
2. Recycled fibers were prone to fail in the vicinity of pit fields and also at points of gross processing induced defects. These fractures could be clearly observed using the ESEM tensile testing technique.
3. Initial observations suggest that secondary wood fibers may display different failure characteristics as compared to virgin fibers. These differences appear to be in the form of increased crack width and premature failure of the S1 layer for recycled fibers.
4. Investigations of micromechanical properties and fracture characteristics of both virgin and recycled fibers are now possible with the ESEM tensile testing technique, but additional testing needs to be conducted to quantify these conclusions. Quantified results may have significance with regard to papermaking and could also help elucidate the structural properties of paper and composites that contain both virgin and secondary fibers. ■

Literature cited

1. Page, D. H., El-Hosseiny, F. E., Winkler, K., and Lancaster, A. P., *Tappi* 60(4): 114(1977).
2. Stokke, D. D., *1992 Materials Research Society Proceedings*, Pittsburgh, vol. 266, Chapter 4.
3. Howard, R. C., *J. Pulp Paper Sci.* 16(5): 143(1990).
4. Wuu, F., Mark R. E., and Perking R. W., *TAPPI 1991 International Paper Physics Conference Proceedings*, TAPPI PRESS, Atlanta, p. 663.
5. Kersavage, P. C., "A System for Automatically Recording the Load-Elongation Characteristics of Single Wood Fibers Under Controlled Relative Humidity Conditions," USDA, U.S. Government Printing Office, Washington, 1973.
6. Ehrnrooth, E.M.L. and Kolseth, P., *Wood and Fiber Science* 16(4): 549(1984).
7. Page, D. H. and Tydeman, P. A., "The Formation and Structure of Paper," Trans. BPBMA Symposium London, 1962, p. 397.
8. Page, D. H. and Seth, R. S., *Tappi* 63(10): 99(1980).
9. Kim, C. Y., Page D. H., El-Hosseiny, F. E., and Lancaster, A. P., *J. Appl. Poly. Sci.* 19: 1549(1975).
10. Page, D. H. and El-Hosseiny, F. E., *Svensk Papperstid.* 14: 471(1976).
11. Page, D. H., El-Hosseiny, F. E., Winkler, K., and Bain, R., *Pulp Paper Mag. Can.* 73(8): 72(1972).
12. Armstrong, J. P., Kyanka, G. H., and Thorpe, J. L., *Wood Science* 10(2): 72 (1977).
13. Cameron, R. E. and Donald, A. M., *Journal of Microscopy* 173:227(1994).
14. Choi D., Thorpe, J. L., and Hanna, R. B., *Wood Science and Technology* 25: 251(1991).
15. Chao, Y. J. and Sutton, M. A., "Computer Vision in Engineering Mechanics," a discussion paper prepared for the NSF Workshop on Solid Mechanics Related to Paper, Blue Mountain Lake, NY, 1986.
16. Wilson, K. and White, D.J.B., *The Anatomy of Wood: Its Diversity and Variability*, Stobart and Son Ltd., London, 1986.
17. Salmen, L. and de Ruvo, A., *Wood and Fiber Science* 17(3): 336(1985).
18. Okayama, T., Yamagashi, Y., and Oye, R., *Japan Tappi* 36(2): 71(1982).

The authors would also like to acknowledge the skilled assistance of Paivi Forsberg and the University of Maine Department of Chemical Engineering Paper Surface Science Laboratory for use of the ESEM. This work was supported in part by McIntyre Stennis project ME09607. The MAFES document number is 1838.

Received for review Feb. 24, 1994.

Accepted Dec. 1, 1994.